Original Research Article

Effect of taper angle on crashworthiness performance in hybrid tubes

Murat Altın

Department of Automotive Engineering, Faculty of Technology, Gazi University, Ankara, 06590, Turkey

ARTICLE INFO	ABSTRACT
	The present paper dealt with the finite element analysis (FE) analyzing the taper angle design of aluminum/E-glass fiber reinforced polymer hybrid tubes. This study investigated the crushing characteristics involving peak crush force (PCF), crush force efficiency (CFE) and specific energy absorption (SEA) capacity of thirty different configurations of hybrid tubes. Three types of geometries were studied numerically, including circular, square and hexagonal. The structures evaluated included circular hybrid tubes fabricated with aluminum alloy and composite. The hybrid structures were subjected to axial impact loads using a 750-kg rigid impactor with an initial velocity of 15 m/s. It was found that the crashworthiness performance increased with increasing taper angle. The SEA and CFE values of the circular hybrid tube with a 10° taper angle were high in the other square and hexagonal hybrid tubes. That hybrid structure can preferable as impact energy absorber due to the ability to withstand axial impact loads effectively.

1. Introduction

Energy absorbing components are important passive safety system elements. These structures are placed between the buffer and the chassis. The cross section geometry and materials of energy absorber structures are various, so, investigating this subject is the aim of many studies.

Metal and composite structures are used in automotive components to absorb substantial amount of deformation energy. Deformation behavior of the metal structures, mostly used in automotive bodies, has been well investigated experimentally [1,2], numerically [3,4] and analytically [5,6]. Composites have wide applications in automotive [7-9], racing car [10,11], aerospace [12,13] and spacecraft industry [14,15]. The composite tubes are used to reinforce the metal tubes and enhance its energy absorption capacity. Hybrid tubes are made from several layers of composites and metals. As an efficient energy absorbing structure, hybrid tubes are widely studied by researchers in recent years.

Researchers have conducted numerical and experimental studies on hybrid tubes of various

cross-sectional geometries. Hybrid tubes can have different geometry profiles, such as circular tubes [16,17], square tubes [18,19], corrugated tubes [20,21] and tapered tubes [22,23]. Kathiresan et al. investigated the low velocity axial impact and quasi-static loading deformation behavior of fiber metal laminated hybrid conical frusta in Ref. [24,25]. Reuter and Tröster [26] investigated the crashworthiness of aluminum and carbon fiber reinforced polymer (CFRP) hybrid tubes. They found that hybrid tubes showed remarkable lightweight potential, and the special energy absorption of the hybrid tubes was 37 % higher than that of pure metal tubes. Zhu et al. [27] researched the absorbed energy capacity of composite, metal and metal/composite hybrid tubes under axial and oblique crushing loading. They found that different crush loading angles have effect on the crash performance of hybrid and other tubes. Mirzaei et al [28] studied circular hybrid tubes under axial crushing loading. They found that hybrid tubes have more energy absorption capacity in comparison to bare metal tubes. Energy absorbing capacity of axial crushing of hybrid tubes around aluminum tubes were numerically investigated by El-Hage et al. [29]. They found that the SEA capacity of the E-glass fiber–epoxy composite tubes was higher than those the other tubes. Costas et al [30] compared the energy absorption of different structures hybrid tubes with tube made of steel, in their study, they found that crashworthiness performance of glass-fiber reinforced polyamide was higher than hybrid tubes. Esnaola et al. [31] had examined quasi-static compression test to study semi-hexagonal cross-section composite fibers. They found that the highest energy absorption values of nearly 30 kJ/kg. Hu et al. [32] investigated the deformation characteristics and crashworthiness performance of hybrid tubes. Their results showed that the hybrid tubes the significantly affects the crashworthiness performance and energy absorption capacity. Zhou et al. [33] investigated the crashworthiness performance of carbon fiber-reinforced dual-phase epoxy–polyurea hybrid composite tubes. They showed that the crashworthiness performance of carbon-fiber reinforced epoxy hybrid tubes is greater than that of other tubes. Song et al [34] experimentally investigated the quasi-static and dynamic impact test on pure metal and FRP metallic structures. They identified four typical collapse modes for tubes including: compound diamond, compound fragmentation, delamination and catastrophic failure.

In the present paper, the effects of taper angle on the crashworthiness performance of hybrid circular, square and hexagonal tubes were numerically investigated. The new design hybrid tube is proved to be a perfect crashworthiness performance with low peak crash force and very high crush force efficiency. It should also be noted that the effect of tapering on hybrid tubes has not been investigated yet in the open literature, and this paper presents a novel contribution in this subject.

2. Problem Description

Thin-walled hybrid tubes having circular, square and hexagonal cross-sections types are focused in this study. The hybrid tubes that were used in the FE analysis contained circular, square and hexagonal cross section. Those hybrid tubes were made of steel, aluminum and composite structure with a wall thickness of 2 mm and length 200 mm (see Figure1.). To research the effect of the taper angle, eleven different taper angle values (0°,1°,2°,3°,4°,5°,6°,7°,8°,9° and 10°) are used. The abbreviation CSCA denotes the circular steel/composite/aluminum models, SSCA denotes the square steel/composite/aluminum models, whereas HSCA denotes hexagonal steel/composite/aluminum models.
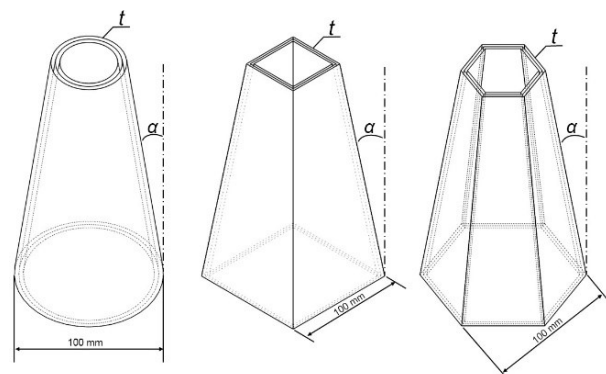

Figure 1. Geometrical configuration

Different parameters have been introduced in FE analysis to evaluate the crashworthiness performance of the structures. The main parameters included in this paper are listed below:

- total energy absorption (T_E)

- specific energy absorption (*SEA*)
- mean crush force (*MCF*)
- peak crush force (*PCF*)
- crush force efficiency (*CFE*)

Total energy absorption (T_E) is the area under the force versus displacement curve. T_E is calculated from:

$$T_E = \int P(s)\,ds \qquad (1)$$

where the parameter P is the force and ds is the cut-off displacement.

The specific energy absorption (*SEA*) is defined as the T_E per unit mass (m) of the profile and is given by:

$$SEA = \frac{T_E}{m} \qquad (2)$$

The mean crush force (*MCF*) can be determined by dividing the T_E by the displacement (L), and is given by:

$$MCF = \frac{T_E}{L} \qquad (3)$$

During the crash, the maximum impact force point gives the peak crush force (*PCF*),

$$PCF = \max(F(s)) \qquad (4)$$

The crush force efficiency (*CFE*) is the *MCF* divided by the *PCF*, or:

$$CFE = \frac{MCF}{PCF} \qquad (5)$$

They are all very important in the crashworthiness criteria of energy absorber tubes. It is desirable that the *PCF* is low *SEA* and *CFE* are at the highest level.

3. Finite Element Modeling

In this study, Ls-Dyna was used to perform all simulations of finite element analysis. The approximate mesh size is set at 3 mm. The hybrid tubes are fixed on a rigid wall where it is impacted by an impact mass of 750 kg, 15 m/s impact velocity as shown in Figure 2. For the composite tube, E-glass/PET199 composite layup was chosen with materials properties listed in Table 1. Mechanical properties of the steel and aluminum tube were entered in the Ls-

Dyna in accordance with the data shown in Table 2. extracted from the engineering stress–strain curve.
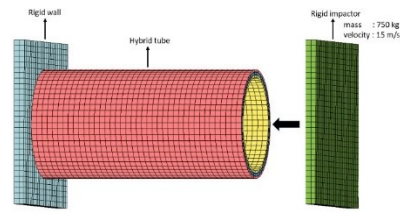

Figure 2. Finite element model of hybrid model

Table 1. Material properties of laminate composite material E-glass/PET199

Property	Description	Value
ρ	Density	2.0 g/cm^3
E_a	Modulus in longitudinal (fiber) direction	37.9 GPa
$E_b = E_c$	Modulus in transverse direction	11.5 GPa
G_{12}	Shear modulus	4.5 GPa
v_{12}	Major Poisson's ratio	0.29
v_{21}	Minor Poisson's ratio	0.0811
X_t	Longitudinal tensile strength	936 MPa
X_c	Longitudinal compressive strength	484 MPa
Y_t	Transverse tensile strength	25.7 MPa
Y_c	Transverse compressive strength	143 MPa
S_c	Shear strength	16.1 MPa
S_b	Inter-laminar shear strength	62.6 MPa
V_f	Fiber volume fraction	70%

Table 2. Material properties of steel and aluminum

Steel		
Property	Description	Value
ρ	Density	7.850 g/cm^3
E	Young modulus	210 GPa
v	Poisson's ratio	0.33
σ_y	Yield strength	304 MPa
Aluminum		
Property	Description	Value
ρ	Density	2.800 g/cm^3
E	Young modulus	70 GPa
v	Poisson's ratio	0.33
σ_y	Yield strength	250 MPa

The dynamic and static coefficients of friction were chosen 0.3 and 0.2, respectively. The contact between the rigid impactor and the hybrid tube is AUTOMATIC_NODE_TO_SURFACE_CON TACT.
AUTOMOTIC_SINGLE_SURFACE_CONTA CT_contact is applied between the hybrid tubes. The contact between the hybrid tube and the rigid wall is A AUTOMATIC_NODE_TO_SURFACE_CON

TACT algorithm. Belytscko-Tsay shell element with five integration points is chosen. However, material of the structures (aluminum and steel) was modeled by MAT_MODIFIED-PIECEWISE- LINEAR-PLASTICITY model MAT-24 in Ls-Dyna. Material applied for the composite tube is composite, which is modeled with the MAT_ENHANCED_COMPOSITE_DAMAGE model MAT-54 in LS-DYNA. The post-processor LSPREPOST is used for visualization and data acquisition.

4. Experimental Validation

Validation of the experimental results is critical for the acceptance of such simulations. This section describes the results of numerical FE simulation of composite tubes are compared with the experimental results. Zhang et al. have carried out experiments for composite circular tube under axial loading [35]. In their experiments they adopted composite E-glass/PET199 structures extruded tubes with lengths of 100 mm, inner diameter of 80 mm and wall thickness 2.4 mm. The comparison of the FE analysis results obtained in this study and the results presented in [35] are given in Table 3. Fig. 3. compares the force-displacement curve results obtained from the experimental [35] and finite element result.

This numerical simulation was compared to metal tubes (steel) sets of the numerical analysis result by Nagel [36]. Table 4. presents crashworthiness parameters of the steel specimens modeled in the studies. Figure 4. depicts a comparison of the deformed shape

between FE analysis and experimental result at crush distance of 200 mm. The finite element results demonstrate that there is a perfect compatibility between numerical results of this paper and mentioned references.
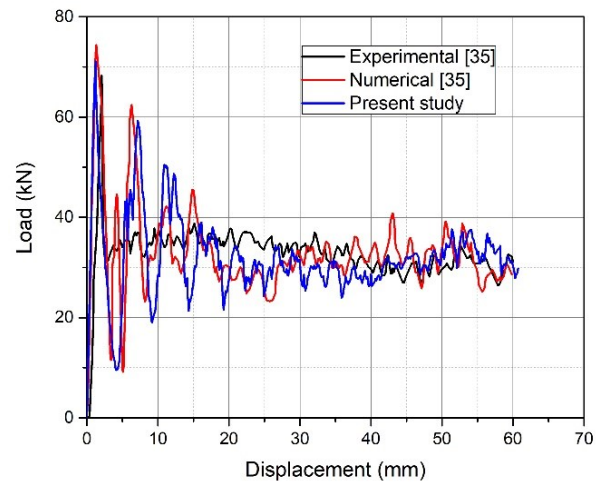

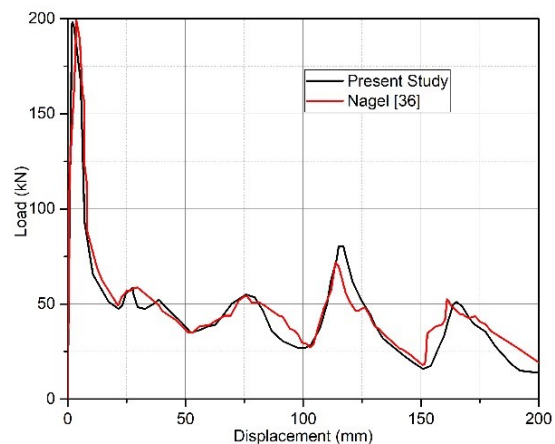Figure 3. Validation of load-displacement curve of composite tube

Figure 4. Validation of load-displacement curve of steel tube

Table 3. Comparison between FE analysis and experimental results for composite tube

	Crush distance (mm)	T_E (kJ)	PCF (kN)	SEA (kj/kg)
Zhang [35]	60	1.968	68.26	14.77
Zhang [35]	60	1.927	74.36	14.47
Present study	60	1.924	71.10	14.44

Table 4. Comparison of FE analysis and experimental results for steel tube

	Crush distance (mm)	T_E (kJ)	PCF (kN)	SEA (kj/kg)
Nagel [36]	200	9.036	199.49	8.53
Present study	200	8.922	198.72	8.42

5. Result and Discussion

In this section, various angles were used for different types of analyses so as to find out the effects of taper angle. The results of the FE analysis are given in Table 5, Table 6 and Table

7, respectively. Table 5. The effect of taper angle on the crashworthiness performance of circular hybrid tubes.

For all the hybrid tubes, the increase in SEA and CFE is almost directly proportional to the increase in tube taper angle. For example, for the

CSCA hybrid tube, the CFE increased from 0.45 to 0.70 when the taper angle increased from 0 to 10 (see Figure 5., Figure 6. and Figure 7.). As for the SEA, it increased from 98.19 kJ/kg to 136.47 kJ/kg when the taper angle increased from 0 to 10 (see Figure 8., Figure 9. and Figure 10.).

The increase in the angle contributed positively to both SEA and CFE. It is clear that all hybrid tapered tubes generally have better SEA and CFE than the straight hybrid tubes, especially at large load angles.

Table 5. The effect of taper angle on the crashworthiness performance of circular hybrid tubes

Run	Crush distance (mm)	T_E (kJ)	PCF (kN)	MCF (kN)	CFE	Mass (kg)	SEA (kj/kg)
CSCA0	120	32.993	615.98	274.94	0.45	0.336	98.19
CSCA1	120	33.316	573.23	277.63	0.48	0.324	102.83
CSCA2	120	34.751	525.20	289.59	0.55	0.311	111.74
CSCA3	120	31.382	489.26	261.52	0.53	0.299	104.96
CSCA4	120	32.022	451.92	266.85	0.59	0.287	111.57
CSCA5	120	32.134	422.51	267.78	0.63	0.275	116.85
CSCA6	120	30.334	395.14	252.78	0.64	0.263	115.34
CSCA7	120	29.803	375.22	248.36	0.66	0.251	118.74
CSCA8	120	29.667	379.52	247.23	0.65	0.239	124.13
CSCA9	120	29.377	360.45	244.81	0.68	0.227	129.41
CSCA10	120	29.340	348.98	244.50	0.70	0.215	136.47

Table 6. The effect of taper angle on the crashworthiness performance of square hybrid tubes

Run	Crush distance (mm)	T_E (kJ)	PCF (kN)	MCF (kN)	CFE	Mass (kg)	SEA (kj/kg)
SSCA0	120	29.461	794.92	245.51	0.31	0.428	68.83
SSCA1	120	28.243	728.52	235.36	0.32	0.412	68.55
SSCA2	120	30.415	679.15	253.46	0.37	0.397	76.61
SSCA3	120	29.691	625.58	247.43	0.40	0.381	77.93
SSCA4	120	29.461	579.00	245.51	0.42	0.366	80.49
SSCA5	120	28.243	519.77	235.36	0.45	0.361	78.24
SSCA6	120	27.078	610.90	225.65	0.37	0.335	80.83
SSCA7	120	26.373	545.81	219.78	0.40	0.320	82.42
SSCA8	120	26.382	481.07	219.85	0.46	0.305	86.50
SSCA9	120	25.674	408.51	213.95	0.52	0.289	88.84
SSCA10	120	24.370	344.71	203.08	0.59	0.274	88.94

Table 7. The effect of taper angle on the crashworthiness performance of hexagonal hybrid tubes

Run	Crush distance (mm)	T_E (kJ)	PCF (kN)	MCF (kN)	CFE	Mass (kg)	SEA (kj/kg)
HSCA0	120	33.373	676.35	278.11	0.41	0.370	90.20
HSCA1	120	33.744	632.12	281.20	0.44	0.357	94.52
HSCA2	120	32.687	590.44	272.39	0.46	0.344	95.02
HSCA3	120	32.111	547.72	267.59	0.49	0.330	97.31
HSCA4	120	31.336	511.52	261.13	0.51	0.317	98.85
HSCA5	120	30.767	476.52	256.39	0.54	0.304	101.21
HSCA6	120	29.762	424.49	248.02	0.58	0.290	102.63
HSCA7	120	29.535	382.64	246.13	0.64	0.277	106.62
HSCA8	120	28.609	354.50	238.41	0.67	0.264	108.37
HSCA9	120	27.756	336.82	231.30	0.69	0.251	110.58
HSCA10	120	26.018	313.93	222.65	0.69	0.237	109.78

In spite of that both of T_E and PCF values are decreasing by taper angle increasing. For instance, for HSCA hybrid tube, T_E increases from 33.373 kJ to 33.744 kJ when the taper angle increases from 0 to 1, but reduces to 30.767 kJ and then to 26.718 kJ when the taper angle further increases to 5 and then to 10. This change depends on the deformation shape of the hybrid tubes. The change in the amount of total energy absorption capacity depending on the taper angle is given in Figure 11., Figure 12. and Figure 13. Similarly, an increase in the taper angle from 1 to 10 resulted in a decrease in the PCF value (see Figure 14., Figure 15. and Figure

16.). The taper angle increased the CFE even more, even though it reduced the total energy absorption.
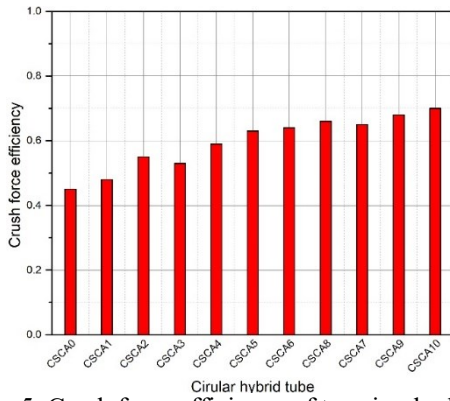

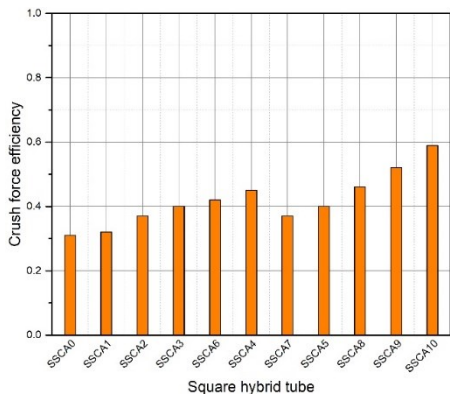Figure 5. Crush force efficiency of ten circular hybrid tubes

Figure 6. Crush force efficiency of ten square hybrid tubes
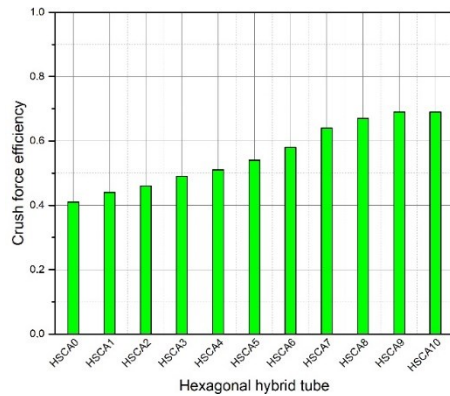

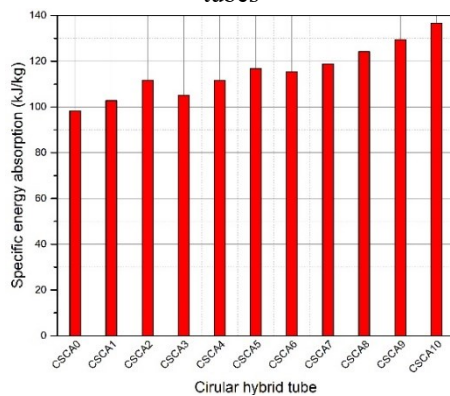Figure 7. Crush force efficiency of ten hexagonal hybrid tubes

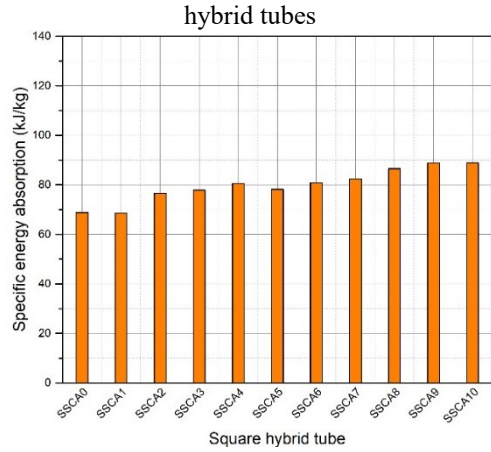
Figure 8. Specific energy absorption of ten circular

Figure 9. Specific energy absorption of ten square hybrid tubes
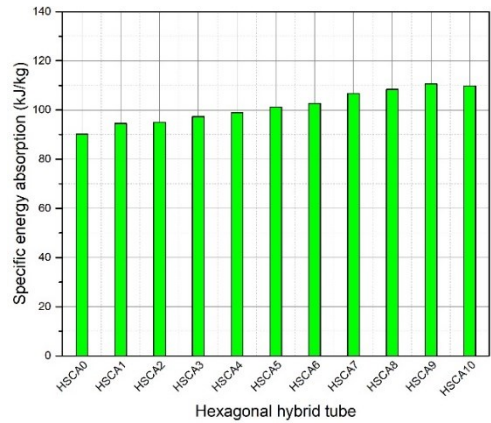

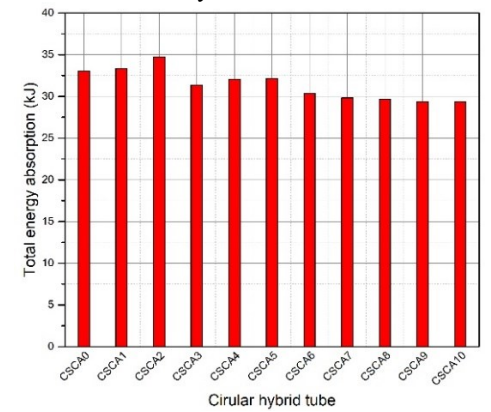Figure 10. Specific energy absorption of ten hexagonal hybrid tubes

Figure 11. Total energy absorption of ten circular hybrid tubes
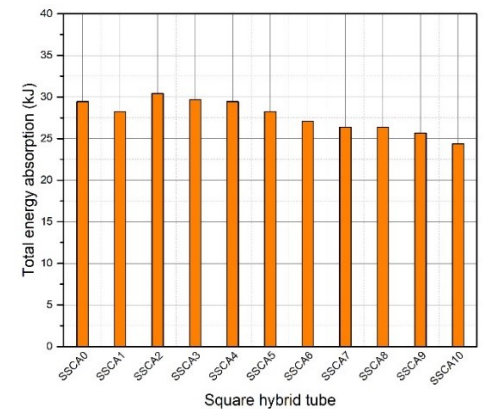

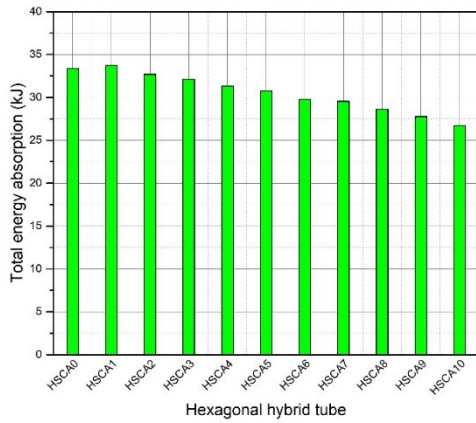Figure 12. Total energy absorption of ten square hybrid tubes

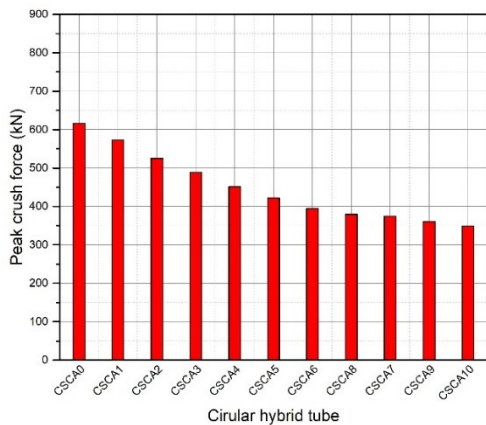Figure 13. Total energy absorption of ten hexagonal hybrid tubes

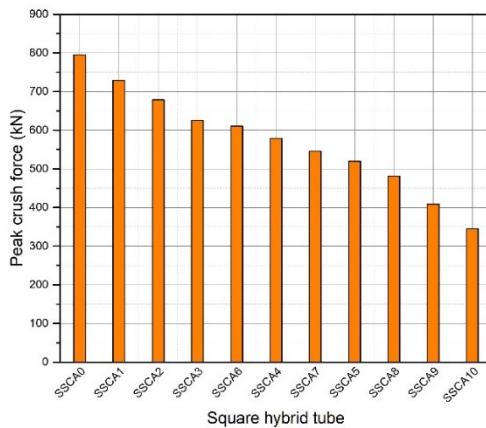Figure 14. Peak crush force of ten circular hybrid tubes

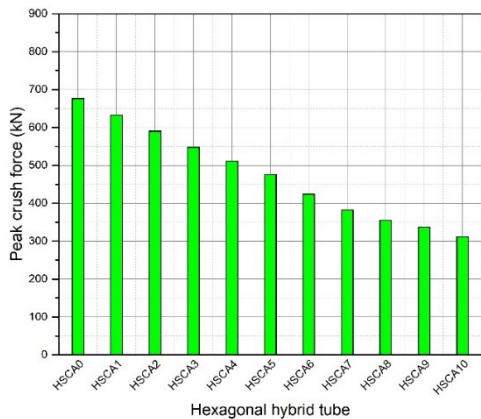Figure 15. Peak crush force of ten square hybrid tubes

Figure 16. Peak crush force of ten hexagonal hybrid tubes

6. Conclusion

This study investigates the crashworthiness of hybrid tubes under dynamic axial impact. From the results obtained, the following conclusions were drawn:

•   Increasing the taper angle from 0° to 10° for the circular, square and hexagonal hybrid tubes gives a decrease in PCF of around 50% for all geometries.

•   Taper angle has significant effect on the TE of hybrid tubes. For circular and square hybrid tubes, TE increased to the point and then continued to decline. For hexagonal, TE continued to decrease as the taper angle increased.

•   It is found for circular, square and hexagonal cross-section hybrid tubes that as the taper angle step by step increases from 0° to 10°, CFE and SAE increase.

•   CSCA10 with 10 ° have highest CFE and SEA under axial impact loading. Specifically, the CFE of the CSCA10 hybrid tube was 226% higher than that of the SSCA0 hybrid tube. Similarly, the SEA of the CSCA10 hybrid tube was 199% higher than that of the SSCA1 hybrid tube.

6. References

1. Mamalis A.G., Manolakos D.E., Loannidis M.B., and P.K. Kostazos, "Axial collapse of hybrid square sandwich composite tubular components with corrugated core: Experimental", International Journal of Crashworthiness, 5(3), 315-332, 2000.
2. Kim H. C., Shin D. K., Lee J. J., and Kwon J. B., "Crashworthiness of aluminum/CFRP square hollow section beam under axial impact loading for crash box application", Composite Structures 112, 1-10, 2014.
3. Mamalis A.G., Manolakos D.E., Loannidis M.B., and Kostazos P.K., "Crushing of hybrid square sandwich composite vehicle hollow bodyshells with reinforced core subjected to axial loading: numerical simulation", Composite Structures, 61 (3), 175-186, 2003.
4. El-Hage H., Mallick P. K., and Zamani N., "Numerical modelling of quasi-static axial crush of square aluminium-composite hybrid tubes", International Journal of Crashworthiness, 9 (6), 653-664, 2004.
5. Shen Q., Wang J., Wang Y., and Wang F.,

"Analytical modelling and design of partially CFRP-wrapped thin-walled circular NCFST stub columns under axial compression", Thin-Walled Structures, 144, 106276, 2019.

6. Mamalis A. G., Manolakos D. E., Demosthenous G. A., and Ioannidis M. B., "Analytical modelling of the static and dynamic axial collapse of thin-walled fibreglass composite conical shells", International Journal of Impact Engineering, 19(5-6), 477-492, 1997.

7. Hesse S. H., Lukaszewicz D. J., and Duddeck F., "A method to reduce design complexity of automotive composite structures with respect to crashworthiness", Composite Structures, 129, 236-249, 2015.

8. Jacob G. C., Fellers J. F., Simunovic S., and Starbuck J. M., "Energy absorption in polymer composites for automotive crashworthiness", Journal of composite materials, 36(7), 813-850, 2002.

9. Bouchet J., Jacquelin E., and Hamelin P., "Static and dynamic behavior of combined composite aluminium tube for automotive applications", Composites science and technology, 60 (10), 1891-1900, 2000.

10. Bisagni C., Di Pietro G., Fraschini L., and Terletti D., "Progressive crushing of fiber-reinforced composite structural components of a Formula One racing car", Composite structures, 68(4), 491-503, 2005.

11. Wang J., Yang N., Zhao J., Wang D., Wang Y., Li K., and Wang B., "Design and experimental verification of composite impact attenuator for racing vehicles", Composite Structures, 141, 39-49, 2016.

12. Wang K., Kelly D., and Dutton S., "Multi-objective optimisation of composite aerospace structures", Composite Structures, 57(1-4), 141-148, 2002.

13. Greenhalgh E., and Hiley M., "The assessment of novel materials and processes for the impact tolerant design of stiffened composite aerospace structures, Composites part A: applied science and manufacturing", 34(2), 151-161, 2003.

14. Morozov E. V., Lopatin A. V., and Taygin V. B., "Design, analysis, manufacture and testing of composite corrugated horn for the spacecraft antenna system", Composite Structures, 136, 505-512, 2016.

15. Lopatin A. V., Morozov E. V., and Shatov A. V., "Axial deformability of the composite lattice cylindrical shell under compressive loading: Application to a load-carrying spacecraft tubular body", Composite Structures, 146, 201-206, 2016.

16. Zhu G., Sun G., Yu H., Li S., and Li Q., "Energy absorption of metal, composite and metal/composite hybrid structures under oblique crushing loading", International Journal of Mechanical Sciences, 135, 458-483, 2018.

17. Zhu G., Sun G., Liu Q., Li G., and Li Q., "On crushing characteristics of different configurations of metal-composites hybrid tubes", Composite Structures, 175, 58-69, 2017.

18. Yu H., Shi H., and Chen S., "A novel multi-cell CFRP/AA6061 hybrid tube and its structural multiobjective optimization", Composite Structures, 209, 579-589, 2019.

19. Shin K. C., Lee J. J., Kim K. H., Song M. C., and Huh J. S., "Axial crush and bending collapse of an aluminum/GFRP hybrid square tube and its energy absorption capability", Composite structures, 57 (1-4), 279-287, 2002.

20. Sokolinsky V. S., Indermuehle K. C., and Hurtado J. A., "Numerical simulation of the crushing process of a corrugated composite plate", Composites Part A: Applied Science and Manufacturing, 42 (9), 1119-1126, 2011.

21. Mamalis A. G., Manolakos D. E., Loannidis M. B., Kostazos P. K., and Papapostolou D. P., "Axial collapse of hybrid square sandwich composite tubular components with corrugated core: numerical modelling", Composite structures, 58(4), 571-582, 2002.

22. Boria S., Scattina A., and Belingardi G., "Axial energy absorption of CFRP truncated cones", Composite Structures, 130, 18-28. 2015.

23. Zhao X., Zhu G., Zhou C., and Yu Q, "Crashworthiness analysis and design of composite tapered tubes under multiple load cases", Composite Structures, 222, 110920, 2019.

24. Kathiresan M., and Manisekar K., "Axial crush behaviours and energy absorption characteristics of aluminium and E-glass/epoxy over-wrapped aluminium conical frusta under low velocity impact loading", Composite Structures, 136, 86-100, 2016.

25. Kathiresan M., Manisekar K., and Manikandan V., "Crashworthiness analysis of glass fibre/epoxy laminated thin walled composite conical frusta under axial compression", Composite Structures, 108, 584-

599, 2014.

26. Reuter C., and Tröster T., "Crashworthiness and numerical simulation of hybrid aluminium-CFRP tubes under axial impact", Thin-Walled Structures, 117, 1-9, 2017.

27. Zhu G., Sun G., Yu H., Li S., and Li Q., "Energy absorption of metal, composite and metal/composite hybrid structures under oblique crushing loading", International Journal of Mechanical Sciences, 135, 458-483, 2018.

28. Mirzaei M., Shakeri M., Sadighi M., and Akbarshahi H., "Experimental and analytical assessment of axial crushing of circular hybrid tubes under quasi-static load", Composite Structures, 94 (6), 1959-1966, 2012.

29. El-Hage H., Mallick P. K., and Zamani N., "A numerical study on the quasi-static axial crush characteristics of square aluminum–composite hybrid tubes", Composite structures, 73 (4), 505-514, 2006.

30. Costas M., Díaz J., Romera L. E., Hernández S., and Tielas A., "Static and dynamic axial crushing analysis of car frontal impact hybrid absorbers", International Journal of Impact Engineering, 62, 166-181, 2013.

31. Esnaola A., Ulacia I., Aretxabaleta L., Aurrekoetxea J., and Gallego I., "Quasi-static crush energy absorption capability of E-glass/polyester and hybrid E-glass–basalt/polyester composite structures", Materials & Design, 76, 18-25, 2015.

32. Hu D. Y., Luo M., and Yang J. L., "Experimental study on crushing characteristics of brittle fibre/epoxy hybrid composite tubes", International journal of crashworthiness, 15 (4), 401-412, 2010.

33. Zhou H., Attard T. L., Dhiradhamvit K., Wang Y., and Erdman D., "Crashworthiness characteristics of a carbon fiber reinforced dual-phase epoxy–polyurea hybrid matrix composite", Composites Part B: Engineering, 71, 17-27, 2015.

34. Song H. W., Wan Z. M., Xie Z. M., and Du X. W., "Axial impact behavior and energy absorption efficiency of composite wrapped metal tubes", International Journal of Impact Engineering, 24 (4), 385-401, 2000.

35. Zhang Z., Sun W., Zhao Y., and Hou S., "Crashworthiness of different composite tubes by experiments and simulations", Composites Part B: Engineering, 143, 86-95, 2018.

36. Nagel G. M., and Thambiratnam D. P., "Dynamic simulation and energy absorption of tapered tubes under impact loading", International Journal of Crashworthiness, 9 (4), 389-399, 2004.